# Modal Analysis of an Aircraft Fuselage Panel using Experimental and Finite-Element Techniques

Gary A. Fleming and Dr. Ralph D. Buehrle,

National Aeronautics and Space Administration
Langley Research Center
Hampton, Virginia 23681, USA

and

Olaf L. Storaasli

Newport News Shipbuilding
Newport News, Virginia 23607, USA

## ABSTRACT

The application of Electro-Optic Holography (EOH) for measuring the center bay vibration modes of an aircraft fuselage panel under forced excitation is presented. The requirement of free-free panel boundary conditions made the acquisition of quantitative EOH data challenging since large scale rigid body motions corrupted measurements of the high frequency vibrations of interest. Image processing routines designed to minimize effects of large scale motions were applied to successfully resurrect quantitative EOH vibrational amplitude measurements from extremely noisy data. EOH and Scanning Laser Doppler Vibrometry (SLDV) results have been used to validate and update finite element models of the fuselage panel. Various modeling techniques were evaluated for characterization of the panel normal modes at frequencies up to 1000 Hz. These models are briefly described, and comparisons between computational predictions and experimental measurements are presented.

*Keywords*: Electro-Optic Holography, EOH, aircraft, fuselage, interferogram, FEM, validation

## 1. INTRODUCTION

NASA's ambitious goal of reducing interior aircraft noise by a factor of two by the year 2007[1] is encouraging the development of advanced instrumentation and analysis techniques. Many interior noise experiments have become increasingly large in size and complexity, increasing the difficulty of acquiring experimental data using accelerometer arrays. These experiments include the detailed measurement of full scale fuselage global bending and torsional modes and examination of the vibroacoustic interactions between fuselage sections. As experiments have grown larger, so too has the number of accelerometers required to obtain the desired dynamic response data and spatial resolution. The undesirable artifacts associated with this increase in accelerometers are: (a) longer setup times; (b) additional measurement uncertainty caused by increased body mass; and (c) the necessity of additional wires, electronics, and data acquisition channels. At the NASA Langley Research Center, Electro-Optic Holography (EOH) is being developed into a tool for routine testing of airframe structures to provide experimental modal analysis capabilities beyond those typically available with accelerometers and Scanning Laser Doppler Vibrometry (SLDV). Advantages of the EOH technique include the ability to acquire image based, non-contacting quantitative measurements of the mean displacement amplitude of a vibrating structure. However, current analysis methods restrict the acquisition of quantitative EOH results to single frequency excitation of the object. It is hoped in the future to extend this technique to provide spectral results of complex waveforms.

Experimental modal analyses of an aircraft fuselage panel under forced excitation were recently performed using EOH and SLDV for finite element model (FEM) validation. The United States Naval Research Laboratory (NRL) used SLDV to establish an extensive database of in- and out-of-plane vibration amplitude measurements for the entire panel. EOH measurements concentrating on the out-of-plane vibrational behavior of the fuselage center bay were obtained at Langley. Results from both experimental methods have been used to validate finite element modeling techniques for the prediction of panel natural mode frequencies and mode shapes to frequencies of 1000 Hz [2]. The EOH technique and its application to measuring aircraft fuselage panels are discussed here. Image processing routines for resurrecting EOH interferograms from extremely noisy data are described, and example results showing the effectiveness of the algorithms are presented. Quantitative displacement amplitude profiles of the panel center bay under forced excitation are presented and compared with FEM predictions of mode shapes and natural frequencies.

## 2. AIRCRAFT FUSELAGE PANEL GEOMETRY

The front and rear sides of the aircraft fuselage panel under investigation are shown in Figures 1a-b respectively. The panel is representative of current aircraft construction but was manufactured without a radius of curvature to simplify experimental measurements and analytical modeling. The 1.2-x 1.8-meter aluminum panel consists of a 1.27 mm skin with six equally spaced longitudinal stringers and four equally spaced vertical frame stiffeners. In an actual aircraft fuselage, the vertical frames are circumferential stiffeners. Rivets attach the stringers and frames to the skin. As shown in Figure 1b, a bay is defined as a section of the panel skin bounded by the stringers and frames. The region-of-interest for EOH measurements was the *center bay*, 191-x 476-mm in size. A piezoelectrically driven inertial shaker was mounted to the stringer at the top of the center bay for forced sinusoidal excitation of the panel at various frequencies and amplitudes. Free-free panel boundary conditions were required to provide a simple boundary that could be applied in the FEM model and physically realized in the experimental setup. To simulate free-free boundary conditions for experimentation, the panel was hung from a test stand using bungee cords attached to each corner. The lack of rigid mounting and size of the panel led to large amplitude (~1 mm), low frequency (0.5-5 Hz) motion of the panel caused by room air currents and floor vibrations. Acquisition of accurate EOH data was impossible under these conditions since panel displacements caused by the rigid body motion far exceeded the 30 μm measurement range of the instrument. Small foam mechanical dampers were devised and applied near each corner of the panel to minimize the rigid body motion. Each damper barely contacted the panel skin to provide minimal structural damping while preserving the forced excitation response characteristics of the center bay. The use of the dampers controlled the panel rigid body motion to tolerable levels for the acquisition of EOH data.

## 3. ELECTRO-OPTIC HOLOGRAPHY MEASUREMENTS

EOH is a well established technique for measuring deformations of statically deformed[3] or dynamically loaded[4] objects. Objects measured using EOH typically have at least one fixed boundary to prevent rigid body motion. This permits measurement of the load induced deformation isolated from other external effects. Although mechanical damping eliminated a majority of the fuselage panel rigid body motion, small amplitude displacements remained which initially corrupted EOH measurements. Advanced image processing algorithms were developed to minimize the effects of the panel rigid body motion on the EOH measurements and permit the determination of quantitative vibration amplitude data. The EOH system and image processing routines used in the current study are discussed in the following sections.

### 3.1 Optical Configuration

The EOH system used in this study is shown schematically in Figure 2, configured for single component, out-of-plane vibration amplitude measurements. The discrete optic and electronic components constituting the actual EOH system are shown in Figure 1a, positioned to measure the vibration amplitudes of the front side of the fuselage panel. A 200 mW continuous-wave (CW), single-frequency laser diode operating at 852 nm was used as the illumination source. Light emanating from the diode passed through several beam shaping and transmit

optics. A Faraday isolator was used to eliminate optical feedback to the laser diode and maintain laser frequency stability. Light exiting the isolator was split into two beams by a plate glass beam splitter. Approximately 90 percent of the light passed through the plate glass beam splitter to constitute the *illumination leg* of the EOH system. The beam splitter first surface reflection was used to construct the *reference leg*. The reference leg and illumination leg optical path lengths were matched to within 10 cm to maximize interference of the coherent laser light. Additional optics were positioned in the illumination leg path to direct the output beam towards the aircraft fuselage panel and expand it to illuminate the center bay. An EOH receiver system consisting of a standard 35 mm SLR camera lens, beam splitter cube, and RS-170 analog video camera was focused to collect laser light scattered from the panel surface. Using a series of mirrors, the reference leg beam was steered through an expanding lens and directed to the EOH receiver beam splitter cube. At the beam splitter cube, scattered light collected by the camera lens was interfered with light from the reference leg. The resulting interference pattern was recorded as a hologram formed on the camera CCD array and was digitized using a PC-based frame grabber.

Two piezoelectrically driven mirrors, or *phase shifters*, were installed in the system for the purposes of optical phase shifting. For vibrating objects, differencing two holograms with a relative 180° optical phase shift produces an *interferogram* containing holographic fringes. The fringe intensity within the resulting image is governed by the Bessel function of the first kind, $J_o$ [4]. The fringes are vibration amplitude contours with a contour interval approximately equal to the laser wavelength (852 nm for the current study). For quantitative analysis of the interferograms, phase shifting was required to eliminate unknowns in the data processing equations so that time averaged vibration amplitude data could be obtained. The phase shifting techniques used for the current work follow those described in reference 4, but have been modified to accommodate the acquisition and processing of ensembles of 64 interferograms at each of 6 phase shift conditions necessary for quantitative analysis. To execute the revised phase shifting technique, the illumination leg phase shifter was modulated at the same frequency as the panel excitation source and was calibrated in phase and amplitude to provide three separate bias modulation settings. At each bias modulation setting, two ensembles of 64 interferograms each were acquired. The reference leg phase shifter was used to induce a 90° optical phase shift between each ensemble, which served to eliminate random optical phase offsets in data processing of the interferograms. The illumination leg bias modulation was necessary to eliminate unknowns in the equations for interpretation of the $J_o$ -related fringes. The six resulting ensembles were used to construct enhanced interferograms as described in Section 3.2 below. The enhanced interferograms were subsequently processed using techniques described in references 3, 4, and 5 for the determination of the vibration amplitude profiles.

### 3.2 Image Processing for EOH Interferogram Enhancement

Quantitative vibration amplitude measurements of the panel center bay at various resonant modes were desired for finite element model validation. Several attempts at obtaining these measurements proved unsuccessful. EOH interferograms of the center bay were poor in contrast and contained fringe patterns distorted by the unrelated panel rigid body motion caused by air currents and movement within the laboratory. Further quantitative analysis of the EOH interferograms required the isolation of the panel bay modes from the rigid body motion. Band pass filtering is the conventional method used for removing the effects of undesired frequency components in a time dependent analog signal. Unfortunately, time domain band pass filtering is not directly applicable to video based data since information at the undesired frequencies is integrated over the exposure time of the CCD camera. Application of mechanical damping near the panel edges reduced rigid body motion to approximately 20 μm amplitude at frequencies ranging from 0.5 to 5 Hz. Since the frequency of these oscillations was much lower than the 30 Hz video rate of the CCD camera, it was reasoned that image processing based on ensembles of images could be used to construct enhanced interferograms containing minimal effects of the rigid body motion.

For each resonant bay mode studied, ensembles of 64 interferograms were acquired at each of 6 optical phase shift conditions necessary for quantitative analysis as described in Section 2.1. The fully three-dimensional rigid body motion of the panel caused portions of the acquired interferograms to be low in contrast and brightness, while regions of the images near the panel instantaneous center of rotation that were subject to minimum panel motion maintained high fringe visibility. For example, the region of highest fringe visibility may have been in the upper left portion of the image for a particular interferogram, whereas it may have been in the lower right portion for another. Calculation of the mean interferogram from each 64 image set yielded interferograms with lower contrast than those within the ensembles and was thus considered an unacceptable method for interferogram

enhancement. Therefore, an algorithm was developed to construct enhanced interferograms from each ensemble based only on those regions within the ensemble having increased contrast and brightness. In this manner, only those portions of the data least affected by the panel rigid body motion were included.

Construction of the enhanced interferogram from each image ensemble began by subdividing each of the 64 images into 64 rectangular subregions, arranged in 8 rows by 8 columns across each image. For discussion, an *(i, j, k)* notation will be followed to describe the subregions, where *i* and *j* denote the subregion row and column respectively, and *k* denotes the interferogram number in the ensemble. For each interferogram *k*, measures of brightness and contrast of each subregion *(i, j)* were determined by calculating the region's integrated pixel intensity and standard deviation. For each subregion *(i, j)* , the series of 64 images was interrogated to determine the 8 brightest corresponding subregions $(i, j, k_B)$ among the ensemble. Pixel values from these 8 brightest subregions $(i, j, k_B)$ were then averaged on a pixel-by-pixel basis over the subregions $k_B$ to create a *brightness optimized* subregion $(i, j)_B$. Finally, the 64 brightness optimized subregions $(i, j)_B$ were reassembled to construct a brightness optimized interferogram $I_B$. An analogous process was performed to determine a *contrast optimized* interferogram, $I_C$. The final enhanced image used for quantitative analysis was computed by:

$$I_E = G * \sqrt{I_B^{\,2} + I_C^{\,2}} \qquad (1)$$

where $I_E$ is the final enhanced interferogram, $G$ is a gain constant, and $I_B$ and $I_C$ are the brightness and contrast optimized interferograms respectively. Thus the value of each pixel *(m, n)* in the final enhanced interferogram was calculated from the values of 16 corresponding pixels *(m, n)* : one from each of the 8 highest brightness and 8 highest contrast subregions containing pixel *(m, n)* .

Typical results from the enhancement process are shown in Figure 3. A raw EOH interferogram of the fuselage panel center bay is shown in Figure 3a. Poor contrast and low amplitude completely mask the presence of holographic fringes present within the data. Figure 3b presents the EOH interferogram of Figure 3a following histogram equalization. Holographic fringes are now apparent, but remain low in contrast and definition. The enhanced interferogram is shown in Figure 3c and demonstrates greatly improved contrast and fringe definition in comparison to Figures 3a-b, permitting further quantitative analysis to be performed.

### 3.3 EOH Measured Results

Quantitative EOH measurements of the fuselage panel center bay mode shapes were obtained at 10 different resonant frequencies from 293.0 Hz to 831.7 Hz. This range of frequencies spanned the desired kilohertz frequency validation range for the panel finite element models. Results from the panel forced at 390.0 Hz are presented in Figure 4, beginning with the enhanced interferogram in Figure 4a, wrapped phase map in Figure 4b, 3-D surface plot in Figure 4c, and amplitude intensity map, Figure 4d. Vibration amplitude intensity maps for the center bay forced at other excitation frequencies are presented in Figure 5. During experimentation, many repeated center bay panel modes were revealed at different excitation frequencies caused by the large number of degrees-of-freedom of the full panel. This is shown by examining the similarities between the measured mode shapes at F = 338.0 Hz, 367.0 Hz, and 420.0 Hz in Figure 5. In general, specific mode shapes were observed over a range of excitation frequencies. The mode shapes presented here correspond with the most dominant observed at the center bay.

## 4. COMPARISONS BETWEEN EXPERIMENTAL MEASUREMENTS AND FEM PREDICTIONS

The primary objective of the finite element modeling was to extend the dynamic analysis capability into the kilohertz region for a complex stiffened aircraft fuselage panel. This included the development of the required modeling techniques and the validation of the finite element predictions with experimental results. The validated modeling techniques will be utilized for future studies of the power flow through the aircraft panel. Power flow analyses[6] identify the dominant paths of energy transfer through the structure. This information can be utilized in the evaluation of mechanical energy paths and to reduce the radiated acoustic energy.

FEM model validation was performed by comparing output of the models with the experimentally measured EOH and SLDV[7] results. EOH and SLDV measurements were used to examine the correlation between: (a) computationally predicted and experimentally measured natural mode frequencies; and (b) computationally predicted and experimentally measured mode shapes. The FEM models were subsequently modified to maximize agreement with experimental results.

### 4.1 Finite Element Modeling Techniques

Geometric and finite element models of the full multi-bay fuselage panel were developed in MSC/PATRAN. The models were generated based on physical dimensions and material properties of the panel specified in manufacturing drawings. Normal mode analysis of the panel finite element models was performed using the Lanczos method in MSC/NASTRAN version 69.

Several methods of modeling the panel were examined in order to meet the objective of characterizing the panel dynamic response though 1000 Hz. First, the required finite element mesh density of the panel skin was evaluated by performing a normal mode analysis of a single bay with clamped boundary conditions. The skin was modeled with linear plate elements. A mesh of 30-by 16-elements was found to provide a one percent convergence on frequency and adequate spatial resolution to define the mode shapes through 1000 Hz. After establishing the model for the panel skin, three methods of modeling the stiffeners were evaluated. The simplest method was to model the stiffeners with *beam* elements. Beam elements are one-dimensional elements having the effective cross-sectional properties of the stiffeners. Beam element stiffeners were defined along lines consistent with the physical rivet lines attaching the actual skin to the stiffeners. The beam stiffener model of the panel contained approximately 60,000 degrees-of-freedom.

Two-dimensional linear *plate* elements were used as a second method of modeling the stiffeners. This required a detailed model of the stiffener geometry. Two variations of the plate element model were investigated. In the first configuration, the stiffener plate elements were modeled as being attached to the skin elements over the entire contact surface. This model was found to be too stiff above 500 Hz when compared to experimental data[2]. For the second variation of the plate element model, plate element stiffeners were modeled as being attached at a line corresponding with the rivet lines on the physical structure. This model constrained all six degrees-of-freedom between the skin and stiffener models along the rivet line, and contained approximately 141,000 degrees-of-freedom.

A third model of the stiffeners, referred to as the hybrid model, was motivated by the work of Grosveld[8]. In this work, beam elements were shown to be sufficient for modeling stiffeners with continuous cross-sections but inadequate for more complex frame sections with cutouts. In order to capture the complex load transmission path around the cutouts, Grosveld developed a hybrid model combining plate and beam elements to represent the frame. A hybrid stiffener model for the aircraft fuselage panel was generated to minimize model complexity and provide the required load path near sections with cutouts. Frame sections with cutouts were modeled using plate elements, while stiffeners with continuous cross-sections were modeled using beam elements. For the hybrid model, the stiffener to skin attachment was along lines corresponding with rivet lines on the physical structure. The hybrid model contained approximately 71,000 degrees-of-freedom.

### 4.2 Comparison with Experimental Data

Normal mode analysis of the panel finite element models with free-free boundary conditions resulted in 400 to 500 modes predicted in the 0 to 1000 Hz frequency range depending on the stiffener model. The local bay modes of the panel are of primary importance here for comparison with the EOH and SLDV data. In subsequent discussions, the *(j, k)* mode shape of a bay will be characterized by "*j*" half sine waves along the horizontal and "*k*" half sine waves along the vertical direction.

Comparative analysis between the experimental results and computational predictions has shown the plate stiffener model with rivet line attachment to be most consistent with experiments. Figure 6 shows resonant bay mode frequencies measured using EOH and SLDV and computationally predicted using this version of the finite element model. As discussed in Section 2.4, specific mode shapes were experimentally observed over a range of frequencies, caused by the large number of degrees-of-freedom of the full panel and complex interactions between individual bays. This frequency occurrence range as measured by SLDV is also plotted for each mode shape in Figure 6. For the SLDV measurements and FEM predictions, discrete data points constituting the line plots correspond with frequencies at which the mode shapes were believed to be most dominant. In general, the computational model follows the experimentally measured trends, but consistently predicts resonant frequencies lower than those experimentally measured. This indicates the simulated panel stiffness was less than the stiffness of the actual physical structure. Additional work to revise the computational models to reflect the true panel stiffness and achieve better agreement with experiments is ongoing.

Figure 7 shows mode shapes of the fuselage panel center bay measured using SLDV and EOH and computationally predicted using the plate stiffener / rivet line attachment model for comparison of experimentally measured and predicted mode shapes. Vibration amplitudes of the experimental data have been normalized by their maximum values since amplitude information was not preserved through the finite element normal mode analysis. The computationally predicted mode shapes match the experimental results obtained both by EOH and SLDV.

## 5. SUMMARY AND CONCLUSIONS

Electro-Optic Holography (EOH) and Scanning Laser Doppler Vibrometry (SLDV) were used for experimental validation and enhancement of finite-element models (FEM) for the prediction of the normal vibration modes of an aircraft fuselage panel. EOH was used to measure the out-of-plane vibration amplitudes of several mode shapes of the aircraft fuselage panel center bay under forced excitation. Initial attempts at using EOH to measure the panel center bay vibration modes proved unsuccessful because of unrelated panel rigid body motion. EOH interferogram acquisition and processing routines were developed to minimize the effects of the large scale motion and enhance the interferograms to enable quantitative analysis. These routines are directly applicable to other scenarios where small amplitude, low frequency structural motions corrupt EOH measurements of the high frequency vibrations of interest. This is often the case when the test specimen and EOH system are not mounted to the same optical table.

Several different finite element models were examined for the purpose of characterizing the aircraft fuselage panel dynamic response at frequencies up to 1 kHz. The best agreement with experimental results was obtained for a model using plate elements to represent the stiffeners with attachment of the stiffeners to the skin along lines consistent with the rivet lines on the physical structure. Modal frequencies predicted by the plate stiffener model with rivet line attachment were consistently lower than those measured, indicating discrepancies between the modeled panel stiffness and the stiffness of the actual structure. Work is ongoing to further enhance the models to attain better agreement with experiments.

## 6. ACKNOWLEDGEMENTS

The authors wish to acknowledge personnel from the United States Naval Research Laboratory, Washington, D.C. for their contributions to this research by performing the SLDV analyses. Portions of this research were funded by grant NAG-1-1684 from the NASA Langley Research Center.

## 7. REFERENCES


1. *Aeronautics and Space Transportation Technology: Three Pillars for Success*, NASA Office of Aeronautics and Space Transportation Technology, 1997.
2. Storaasli, Olaf L., "Correlation of Finite Element Prediction and Experimental Measurements of Aircraft Panel Structural Acoustics," M.S. Thesis, Department of Aerospace Engineering, Old Dominion University, 1997.
3. Pryputniewicz, R.J., course notes from "Holographic Numerical Analysis", CHSLT - Worcester Polytechnic Institute. January, 1992.
4. Pryputniewicz, R.J., and Stetson, K.A., "Measurement of Vibration Patterns using Electro-Optic Holography", *Proc. SPIE* **1162,** 456-467 (1989).
5. Takeda, M., Ina, H., and Kobayashi, S., "Fourier-transform method of fringe-pattern analysis for computer-based topography and interferometry," *J. Opt. Soc. Am.*, **60**(1), 156-160 (1972).
6. Gavric, L., and Pavic, G., "A Finite Element Method for Computation of Structural Intensity by the Normal Mode Approach," *Journal of Sound and Vibration*, **164**(1), pp. 29-43, June, 1993.
7. EOH and FEM analyses were performed at NASA - Langley Research Center. SLDV measurements were acquired at the United States Naval Research Laboratory, Washington, D.C., USA.
8. Grosveld, Ferdinand W., "Structural Normal Mode Analysis of the Aluminum Testbed Cylinder (ATC)," AIAA Paper No. 98-1949 to be presented at the *39th AIAA/ASME/ASCE Structures, Structural Dynamics, and Materials Conference*, Long Beach, California, April 20-23, 1998.

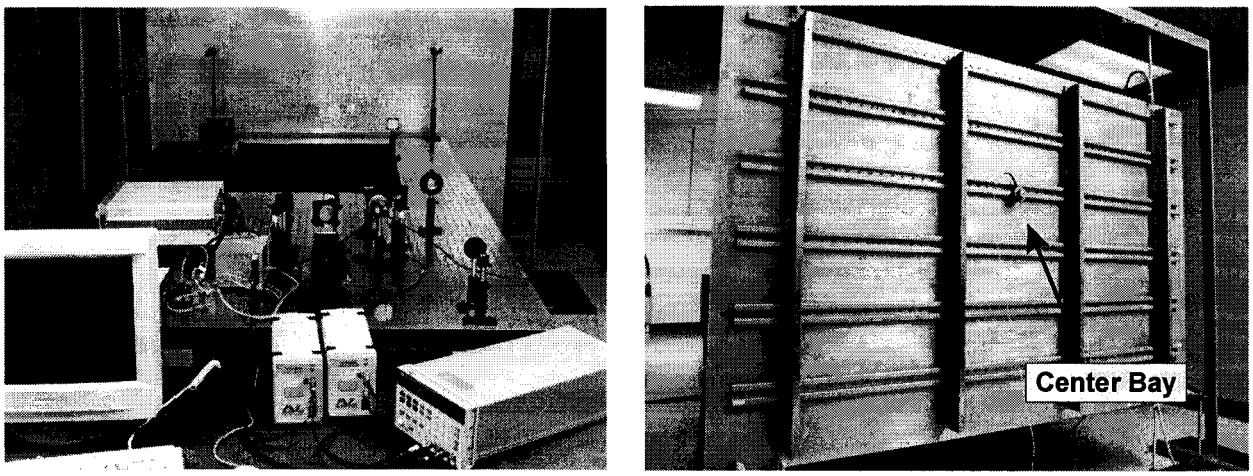


(a) Instrument Configuration

(b) Panel Infrastructure

*Figures 1a-b:* Front and rear sides of the aircraft fuselage panel. Figure 1a also shows EOH instrument configuration.

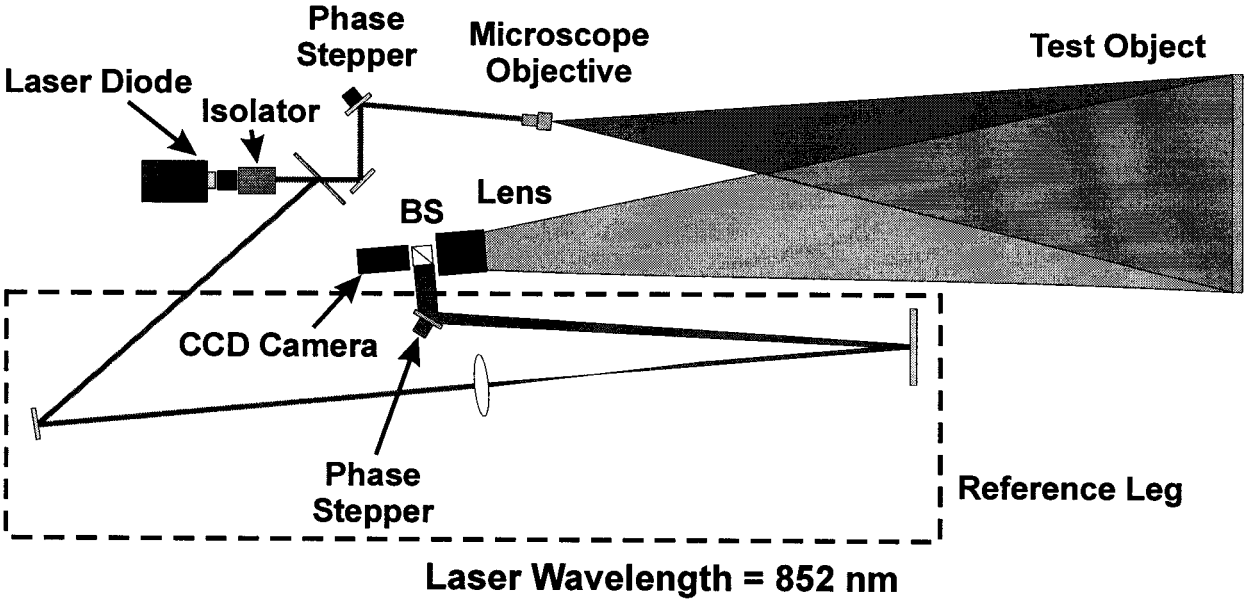


*Figure 2:* Schematic of EOH system optical configuration.

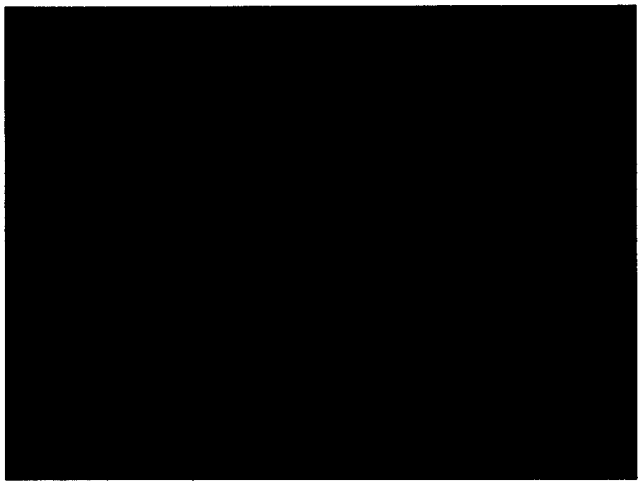

***Figure 3a:*** Raw EOH interferogram of aircraft fuselage panel center bay.

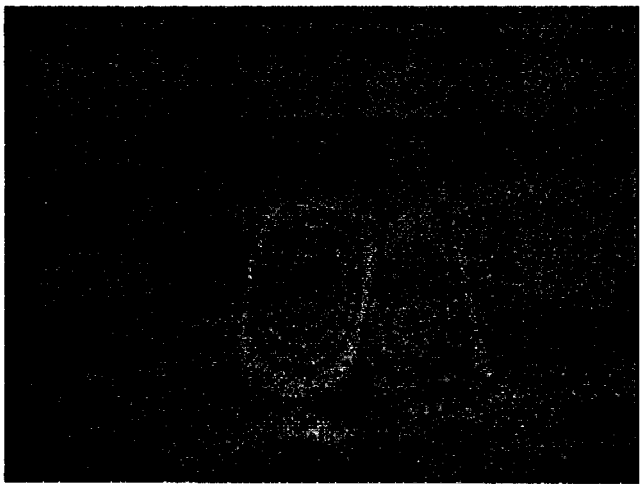

***Figure 3b:*** Raw EOH interferogram following histogram equalization. Holographic fringes are apparent, but corrupted by noise.

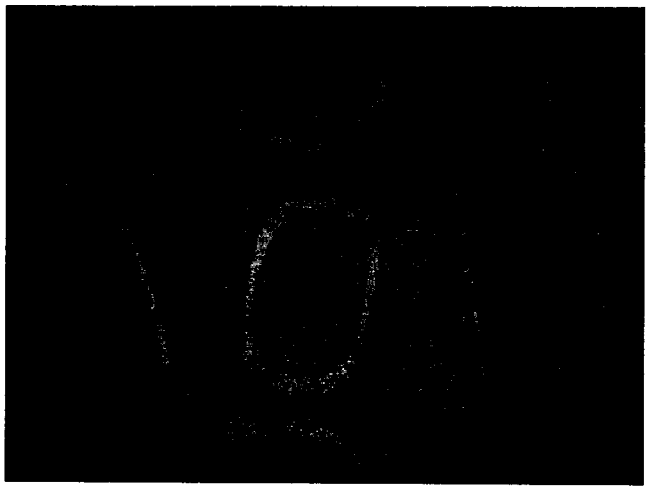

***Figure 3c:*** Enhanced EOH interferogram after brightness and contrast optimization.

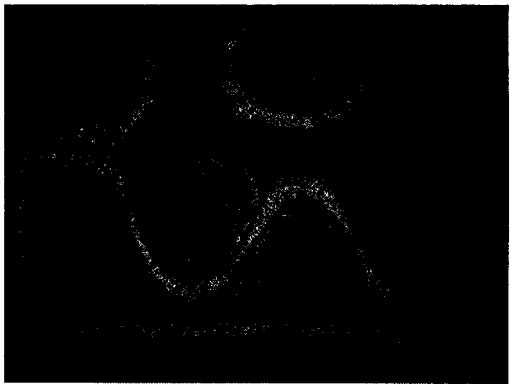

(a) Enhanced Interferogram

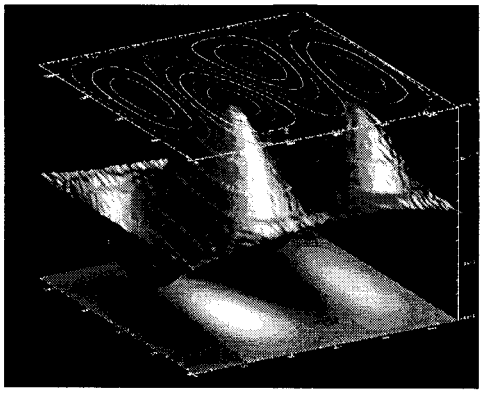

(c) Surface Plot

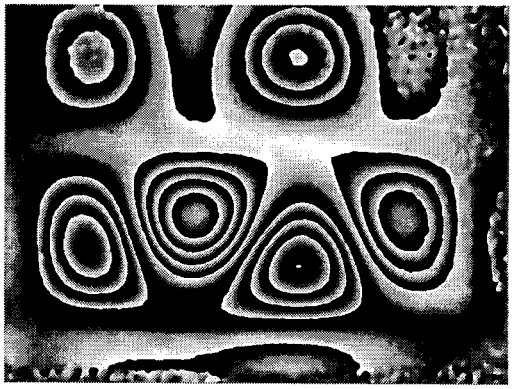

(b) Wrapped Phase Map

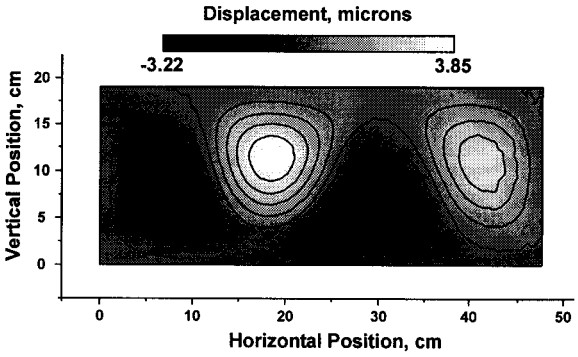


(d) Displacement Contours

*Figures 4a-d*: Example EOH results of the aircraft fuselage panel center bay.

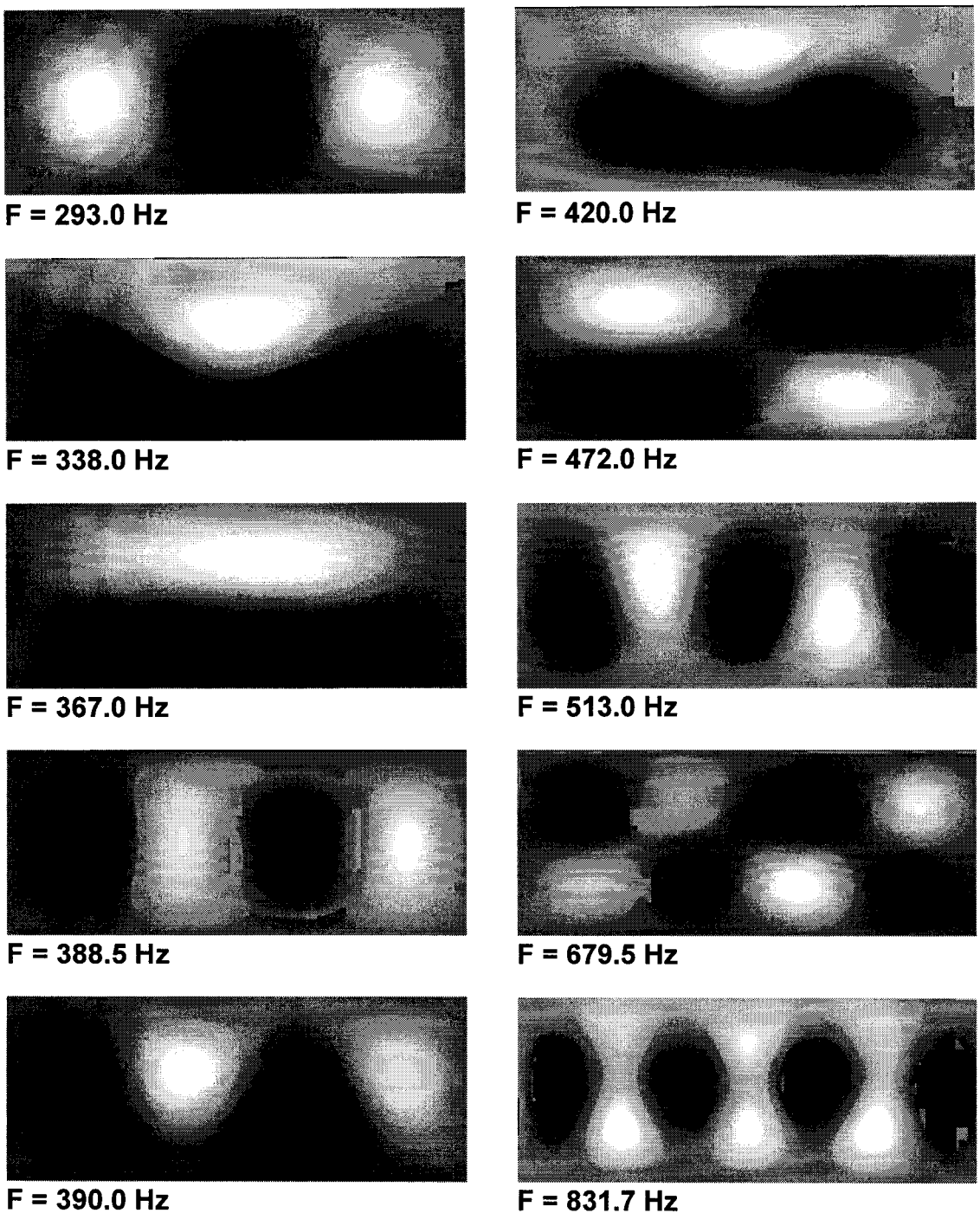


*Figure 5:* EOH measured normalized vibrational amplitude maps of the aircraft fuselage panel center bay.

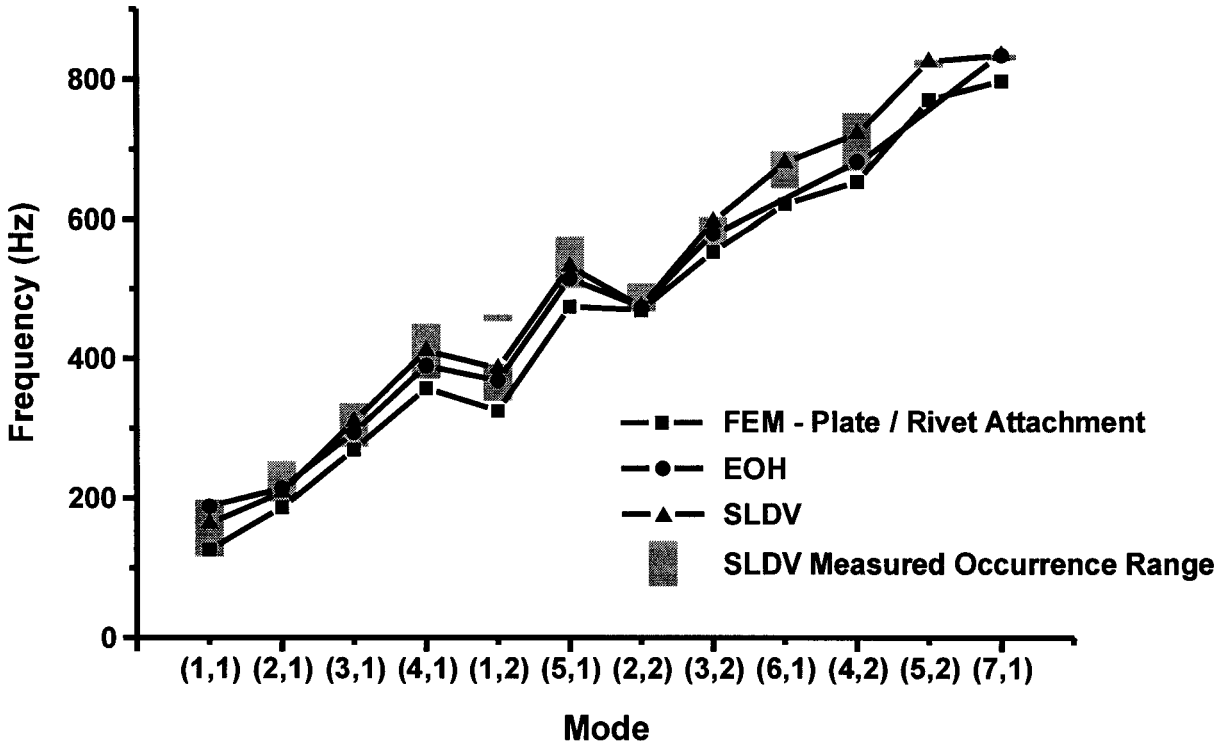


*Figure 6:* Resonant mode frequency occurrence measured by EOH and SLDV and FEM predicted using a plate stiffener / rivet attachment model.

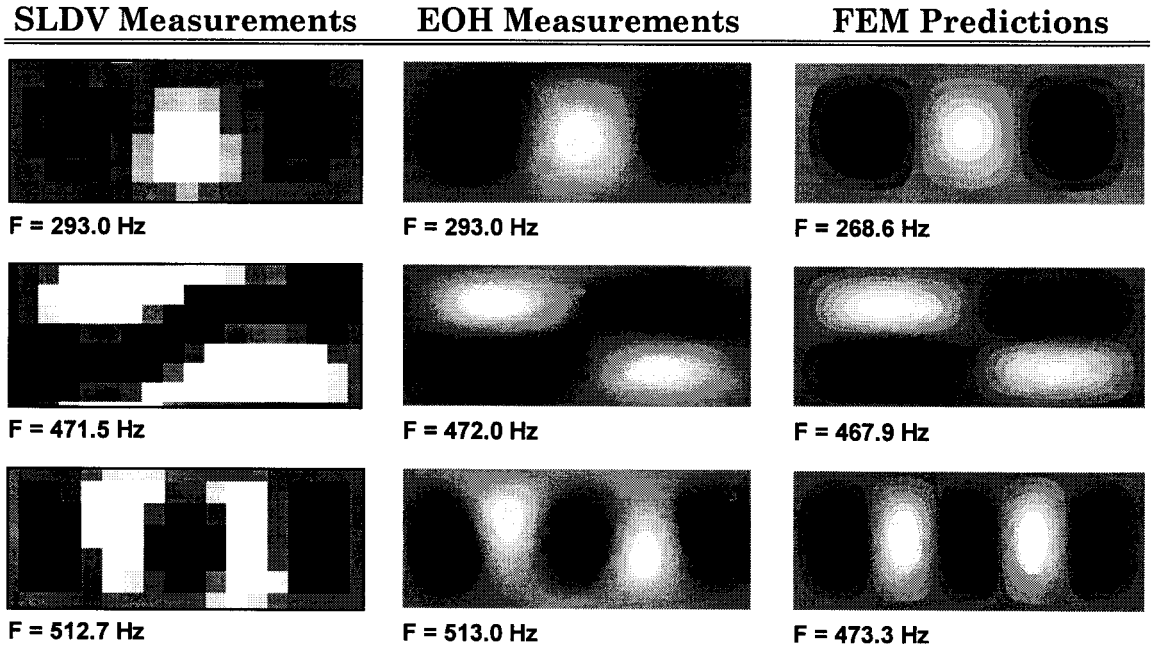


*Figure 7:* Mode shape comparision between experimentally measured and computationally predicted vibrational modes of the center bay.